A channel model for the propagation of X-band radio waves through the solar corona

A.J. Stocker[(1)], D.R. Siddle[(1)], E.M. Warrington[(1)], G. Mariotti[(2)(5)], D. Silvestri[(2)(6)], A. Zeqai[(2)], P. Tortora[(2)], A. Argyriou[(3)], J. De Vicente[(4)], R. Abello[(4)], and M. Mercolino[(4)]

[(1)] University of Leicester, U.K. (sto@le.ac.uk), [(2)] University of Bologna, Italy, [(3)] University of Thessaly, Greece, [(4)] ESA, Darmstadt, Germany, [(5)] Now at SITAEL S.p.A., [(6)] Now at Unisorting S.r.l.

Keywords: radio channel, solar corona, X-band

Abstract

Spacecraft communication systems operating at X-band are strongly affected when the propagation path passes close to the sun (characterised by the Sun-Earth-Probe, SEP, angle). In this paper, a channel model that can generate a time-series of signal amplitude and phase is presented. The channel model reproduces the observations well for SEP>2° and, with some caveats, works at smaller values of SEP.

1 Introduction

When the propagation path between the Earth and a distant spacecraft lies close to the sun, as it does during superior solar conjunctions (Figure 1), the coronal plasma can have severe effects on the communications channel through, for example, the introduction of amplitude and phase scintillations. While much work in this area concentrates on using the effects on signals to diagnose the condition of the solar plasma [1,2,3] other studies have studied the effect on communication systems [4,5,6] usually based on modelling the effects using a Rician distribution.

In this paper, a channel model based on experimentally derived power spectral densities for the phase and amplitude of X-band signals propagating through the solar corona during conjunction is described. An approach has been adopted whereby the behaviour of the power spectral density of the measurements is modelled. For X-band, the results from the model are in close agreement with experimental observations at SEP>2° and, for some purposes, may be suitable down to SEP~1°.

2 Experimental observations

In order to derive the model, open-loop measurements of X-band signals radiated from the Mars Express spacecraft recorded during the Mars solar-conjunction of 2013 while SEP<10° (4 March–26 May) were used. Example measurements of signal power and phase (corrected for orbital dynamics) when SEP~2.4° are presented in Figure 2. The solar plasma causes the relatively low frequency amplitude scintillation and variations in phase while the faster variations are due to the thermal noise.

An example PSD spectrum of the amplitude scintillation is presented in Figure 3. Three main parts to the spectrum have been identified: thermal white noise at frequencies higher than about 10 Hz, a second 'white noise' region between approximately 3×10^{-4} and 0.3 Hz that corresponds to the scintillation introduced by the solar corona, with a transition region (i.e. between 1 and 10 Hz) between them, and pink noise at lower frequencies (this is more evident for higher values of SEP than in this example). In order to model and synthesise the amplitude PSD, separate functions for the pink noise (P_{PN}), solar plasma (P_{GM}), and thermal white noise (P_{WN}) have been combined and the least squares found in an iterative fit for different values of SEP such that

$$P = P_{PN}(f) + P_{GM}(f) + P_{WN} \qquad (1)$$

The frequency spectrum of the phase fluctuations is calculated following the method of [1]. The phase scintillation PSD intensity, $P\phi$ has a form as follows (see Figure 3)

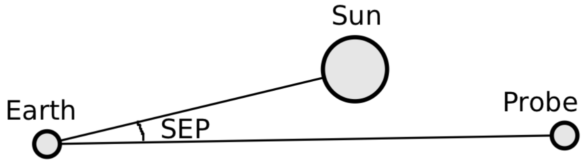

Figure 1: Geometry of Earth and spacecraft during superior solar conjunction

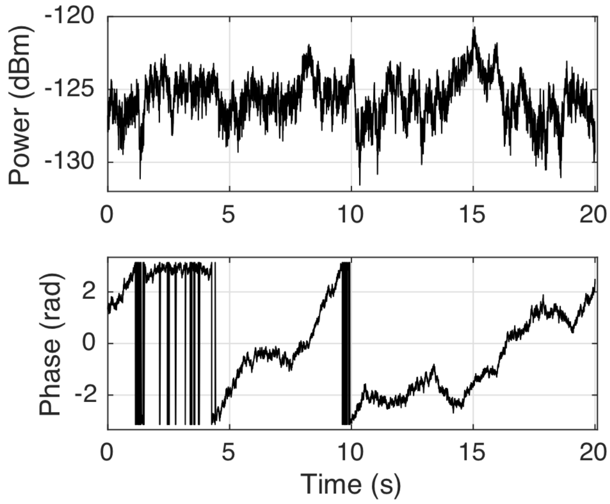

Figure 2: (top panel) Signal power at the input to receiver and (bottom panel) phase observed on 7 April 2013 (SEP~2.4°). A low-pass filter has been applied to the open loop data with a cut off of 200 Hz

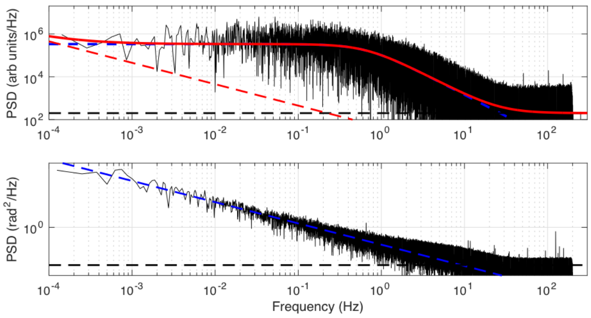

Figure 3. Power spectral density for (top panel) power and (bottom panel) phase on 7 April 2013 (SEP~2.4°). In the top panel, P_{GM} (blue dashed), P_{PN} (red dashed), P_{WN} (black dashed) and P (red solid) are presented. In the bottom panel, $P\phi$ (blue dashed) and $P\phi_{WN}$ (black dashed) are shown.

$$\log_{10}P_{\phi} = m\log_{10}f + c \qquad (2)$$

where, f is the fluctuation frequency and m and c are the gradient and intercept, respectively. A thermal white noise component is also present ($P\phi_{WN}$) in the PSD.

3 Model results

A synthetic time-series of power or phase samples can be generated as follows: first, the PSD (a curve like the overall line in Figure 3) is constructed using the parameters for a given SEP with the desired sample rate and duration (i.e. the inverse of the lowest frequency). The time series is then produced by taking the inverse FFT of the PSD noting that a different time series can be created each time the model is run by randomising the phase of each sample in the PSD spectrum. Some examples of the outcome of this process for the same conditions as for the observations presented in Figure 2 are presented in Figure 4. These time series are highly reminiscent of the ones observed and they have similar properties, e.g. the experimental value of the amplitude scintillation index is 0.34, while the simulated value is 0.36.

4 Concluding remarks

A channel model for X-band signals propagating through the solar corona has been derived from the behaviour of experimentally determined power spectral densities of the variation in signal amplitude and phase. The time series of amplitude and phase obtained from the model have similar characteristics (e.g. amplitude scintillation index, signal distributions, etc.) to the observed values. The results can be scaled to other frequencies (e.g. S-band and Ka-band) and to other systems (e.g. by changing the SNR). However, there are limits to the applicability of the model. For example, the model currently does not include the phase slips associated with deep fades during strong scintillation. However, for X-band, this is not likely to be a problem for SEP>2.1° since this is the highest value of SEP for which phase slips are present in the observations. For lower values of SEP, the model will currently produce over-optimistic performance data since, for example, the phase slips will cause significant errors in the tracking

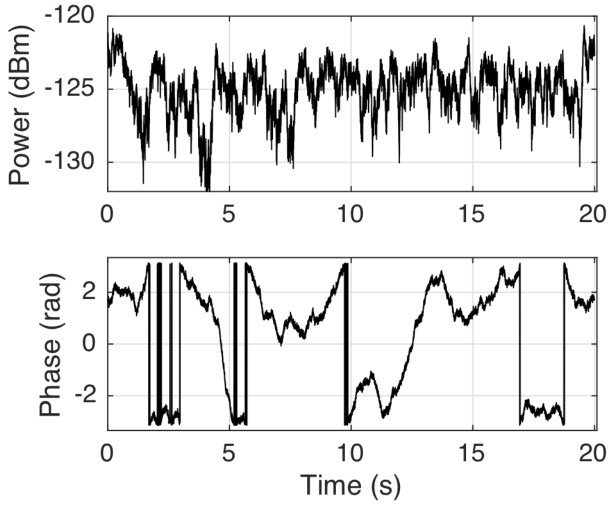

Figure 4: Synthetic time series of (top panel) signal power and (bottom panel) phase for a ‘poor’ channel at SEP=2.4°. The sample rate is 400 samples per second.

capability of a PLL. Another problem with the model for conditions of strong scintillation arises from the Gaussian distributions in amplitude produced by the PSD method since, for these conditions, these should be skewed.

Acknowledgements

This work has been funded by the General Study Programme (GSP) of the European Space Agency

References

[1] R. Woo, F.C. Yang, and K.W. Yip, “Measurements of large-scale density fluctuations in the solar wind using dual-frequency phase scintillations”, *The Astrophysical Journal*, **210**:568–574, (1976).

[2] M. Pätzold, *et al.*, “Coronal density structures and CMEs: Superior solar conjunctions of Mar Express, Venus Express, and Rosetta: 2004, 2006, and 2008”, *Solar Phys* **279**:127-152, DOI 10.1007/s11207-012-9991-y, (2012).

[3] A.K. Verma, *et al.*, “Electron density distribution and solar plasma correction of radio signals using MGS, MEX, and VEX spacecraft navigation data and its application to planetary ephemerides”, *Astronomy and Astrophysics* **550**, DOI: 10.1051/0004-6361/201219883, (2012).

[4] D.D. Morabito, *et al.*, “The Cassini 2000 solar conjunction”, *IEEE Trans. on Antennas and Propagation*, **51**, 201–219, DOI 10.1109/TAP.2003.809055, (2003).

[5] D.D. Morabito, “Solar-induced fluctuations on spacecraft signal amplitude observed during solar superior conjunctions of the Cassini spacecraft”, *Radio Sci*, **42**, RS3002, doi:10.1029/2005RS003425, (2007).

[6] Q. Li *et al.*, “Performance study of a deep space communications system with low-density parity-check coding under solar scintillation”, *International Journal of Communications*, **6**, (2012).